DISCRETE ELEMENT PARAMETER CALIBRATION AND OPTIMIZATION OF LAMINARIA JAPONICA BASED ON GP-PSO-XGBOOST MODEL

/

基于 GP-PSO-XGBOOST 模型的海带离散元参数校准与优化

Xian WANG[1,2,3], Hua ZHOU[*1,2,3], Duanyang GENG[1,2,3], Zehao ZHA[1,2,3], Zhengzhong LI[1,2,3]

[1]School of Agricultural Engineering and Food Science, Shandong University of Technology, Zibo/China.

[2] Institute of Modern Agricultural Equipment, Shandong University of Technology, Zibo/ China.

[3] Key Laboratory of Smart Agriculture Technology and Intelligent Agricultural Machinery Equipment for Field Crops in Shandong Province, Zibo / China.

Tel: +8615071529850; E-mail: zhouhua688@163.com

DOI: https://doi.org/10.35633/inmateh-76-54

Keywords: *Laminaria japonica, DEM, parameter calibration, simulation, XGBoost*

ABSTRACT

During the mechanized harvesting of Laminaria japonica, it is prone to breakage and damage, resulting in an increased loss rate. To accelerate the optimization of harvesting equipment for Laminaria japonica, this study established a simulation model based on the discrete element method. The Hertz-Mindlin with Bonding contact model was used, and parameters of Laminaria japonica were calibrated through shear tests. Using the maximum shear force (F_{max}) as the test indicator, the optimal parameters were obtained through Plackett-Burman test, the steepest climb test, Box-Behnken test, and the GP-PSO-XGBoost regression prediction model. The results indicated that when the coefficient of restitution of Laminaria japonica-steel was 0.45, the normal stiffness per unit area was 303 MN/m³, the shear stiffness per unit area was 378 MN/m³, and the bonding radius was 0.70 mm, the relative error of F_{max} was 0.75%. The average error of the F_{max} for samples at different thicknesses was 3.09%, and the relative error of the maximum puncture force in puncture test was 5.59%. Finally, a discrete element model of the whole Laminaria japonica was established. This study offers theoretical support for the development and optimization of harvesting equipment for Laminaria japonica.

摘要

海带在机械化采收过程中易出现破损和损伤，造成损失率增加。为了加速海带机械收获设备的研发，本研究基于离散元法建立了海带仿真模型。研究采用 Hertz-Mindlin with Bonding 接触模型，通过剪切试验对海带进行参数标定。以最大剪切力（F_{max}）为试验指标，通过 Plackett-Burman 检验、最陡爬坡检验、Box-Behnken 检验和 GP-PSO-XGBoost 回归预测模型得到最优参数。结果表明：当海带钢的恢复系数为 0.45，单位面积法向刚度为 303 MN/m³，单位面积剪切刚度为 378 MN/m³，粘接半径为 0.70 mm 时，F_{max} 的相对误差为 0.75%。不同厚度样品的 F_{max} 平均误差为 3.09%，穿刺试验中最大穿刺力的相对误差为 5.59%。最后，建立海带整体的离散元模型。本研究为海带收获设备的研发与优化提供理论支持。

INTRODUCTION

Laminaria japonica is rich in bioactive components such as fucoidan, mannitol, and iodine*(Li et al., 2023)*, making it a vital raw material in industries like pharmaceutical, healthcare, chemical, and agriculture *(He et al., 2020; Zhao et al., 2024)*. With the growing global demand for *Laminaria japonica*, its production has also been steadily rising *(Naylor et al., 2021)*. Against this backdrop, the development of mechanized harvesting equipment for *Laminaria japonica* is gradually becoming key to enhancing production efficiency and promoting the sustainable development of the *Laminaria japonica* industry *(Chang et al., 2018; Jiang et al., 2022; Tan et al., 2020)*. However, *Laminaria japonica* possesses unique morphological characteristics of being flat and flexible, which often leads to the issue of breakage and damage during the mechanical harvesting process. Addressing this challenge necessitates precise characterization of *Laminaria japonica*'s micromechanical fracture behavior.

Xian Wang, bachelor degree; Hua Zhou, Ph.D.; Duan-yang Geng, Prof. Ph.D.; Ze-hao Zha, bachelor degree; Zheng-zhong Li bachelor degree.*

The discrete element method (DEM) has proven effective in simulating the micromechanical behavior of particle-based materials *(Wachem et al., 2020; Zhao et al., 2023)* and has been widely applied in the mechanical modeling of various crops in agricultural engineering *(Gao et al., 2023; Tang et al., 2023)*. For example, the Hertz-Mindlin with bonding model has been used to construct breakable bonding models for tobacco leaves *(Tian et al., 2023)*, banana stems *(Guo et al., 2021)*, and wheat straw *(Li et al., 2024)*, with parameter calibration conducted through compression, shear, and three-point bending tests. These studies have provided key mechanical parameters for the design and development of harvesting and post-processing equipment. However, despite the extensive application of DEM in modeling terrestrial crops, research on aquatic macroalgae such as *Laminaria japonica* remains limited. Its markedly different mechanical behavior compared to terrestrial crops calls for further investigation into its fracture mechanisms.

This study aims to establish a damageable flexible model of *Laminaria japonica* based on the DEM. By integrating physical tests and simulation analysis, the fracture mechanism of *Laminaria japonica* is investigated. First, physical tests were conducted to determine the intrinsic parameters, contact parameters, and basic mechanical properties of *Laminaria japonica*, based on which a biomechanical model was developed. The Plackett-Burman design was employed to screen key parameters, followed by refinement of the parameter range using the steepest ascent method and Box-Behnken design. To improve calibration efficiency, a hybrid GP-PSO-XGBoost algorithm was introduced to construct a parameter prediction model. The accuracy of the model was validated through shear and puncture tests on *Laminaria japonica* of varying thicknesses. The results not only provide new insights into the study of the fracture mechanics of *Laminaria japonica*, but also offer theoretical support for the design and optimization of *Laminaria japonica* harvesting equipment.

MATERIALS AND METHODS

Sample preparation

The *Laminaria japonica* samples selected for this study were sourced from the Ailun Bay marine ranch in Rongcheng, Shandong, China. The variety used is the No.205 at maturity, which is the primary species cultivated in Rongcheng. The *Laminaria japonica* is divided into upper, middle, and lower sections, as shown in Fig. 1.

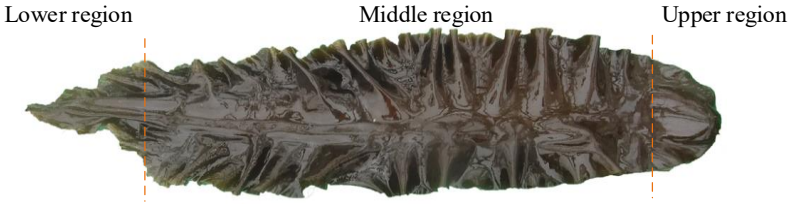

Fig. 1 - The structure of fresh *Laminaria japonica*

During the harvesting process, it was observed that the middle section is the most susceptible to damage. Therefore, the middle section was selected as the research object for preparing *Laminaria japonica* samples for mechanical property analysis.

To acquire representative mechanical performance data, ten mature *Laminaria japonica* specimens were randomly selected, from which two types of rectangular test samples—sample 1 and sample 2—were prepared. Sample 1 measured approximately 80 × 33 mm (length × width), with a total of 40 samples produced; sample 2 measured approximately 10 × 10 mm, with 10 samples prepared in total, as shown in Fig 2. The thickness of each sample 1 was measured using a digital caliper, with a range from 0.8 to 5.2 mm.

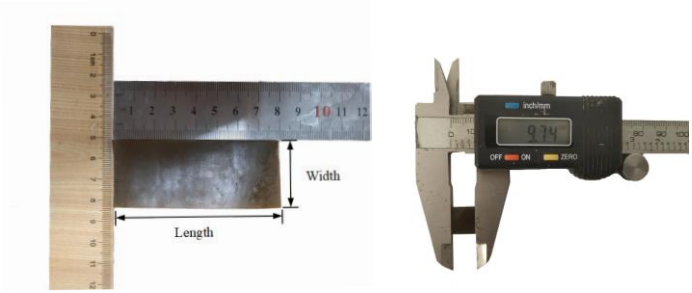

(a) sample 1 *(b) sample 2*

Fig. 2 - Test sample of *Laminaria japonica*

Density measurement

Since there is no reference for the density of *Laminaria japonica*, it was measured using the pycnometer method. The pycnometer was cleaned, dried, and filled with distilled water, then weighed using a JCS-Z1 electronic balance (accuracy: 0.1 g). Subsequently, the *Laminaria japonica* was cut into uniform pieces and weighed. The *Laminaria japonica* was gently placed into the pycnometer, and any overflowed water was carefully wiped off with absorbent paper. The total mass of the pycnometer was measured again (Fig 3a). The density of the *Laminaria japonica* was calculated as follows:

$$\rho_g = \frac{m_g}{m_p + m_g - m_z}\rho_s \tag{1}$$

where: m_g is the mass of *Laminaria japonica* in air, kg; ρ_g is the density of *Laminaria japonica*, kg/m^3; ρ_s is the density of distilled water at room temperature, kg/m^3; m_P is the mass of the pycnometer filled with water, kg; and m_z is the total mass of the pycnometer containing the remaining water and *Laminaria japonica* after the overflowed water is wiped off, kg.

After multiple experiments, the density of *Laminaria japonica* was calculated to be 1263 kg/m^3.

Poisson's ratio and shear modulus

In this study, the multifunctional texture analyzer (ENS-DVU, range: 1000 N, accuracy: 0.01 N, Beijing Enovation Technology Development Co., Ltd.) (Fig 4a) was used to perform compression tests on sample 2 to determine the Poisson's ratio (v) and shear modulus (K) of *Laminaria japonica*, as shown in Fig 3b. The Poisson's ratio of *Laminaria japonica* was calculated using Eq (2).

$$v = \left|\frac{\varepsilon_1}{\varepsilon_2}\right| = \frac{L_1 - L_2}{H_1 - H_2} \tag{2}$$

where: ε_1 is the strain perpendicular to the load direction, ε_2 is the strain in the direction of the applied load, L_1 is the lateral dimension before compression, mm; L_2 is the lateral dimension after compression, mm; H_1 is the axial dimension before compression, mm; and H_2 is the axial dimension after compression, mm.

The shear modulus (K) can be calculated using Eq (3).

$$K = \frac{F \cdot L}{2(1+v) \cdot S \cdot \Delta L} \tag{3}$$

where: F is the maximum load during the elastic deformation phase of the test sample, N; L is the initial length of the test sample, mm; S is the cross-sectional area of the test sample, mm^2; and ΔL is the change in length before and after compression, mm.

After multiple tests, the Poisson's ratio of *Laminaria japonica* was determined to be 0.338, and its shear modulus was calculated as 5.43 MPa.

Coefficient of friction and coefficient of restitution

The coefficient of restitution of *Laminaria japonica*-steel ($COR_{L\text{-}S}$) was measured using a collision bounce test. A high-speed camera was used to record the collision between the *Laminaria japonica* and the steel plate (Fig.3c), and the coefficient of restitution (e) was calculated using Eq (4). The coefficient of restitution of *Laminaria japonica-Laminaria japonica* ($COR_{L\text{-}L}$) was measured using the fine wire suspension method (Fig.3d). The friction coefficient was measured using a friction tester (Fig 3e).

$$e = \left|\frac{v'}{v}\right| = \sqrt{\frac{2gh}{2gH}} = \sqrt{\frac{h}{H}} \tag{4}$$

where:

h is the height at which *Laminaria japonica* bounces up after falling, mm; H is the initial height of *Laminaria japonica*, mm.

After conducting multiple experiments, the average $COR_{L\text{-}L}$ and $COR_{L\text{-}S}$ were calculated to be 0.38 and 0.48, respectively. The average coefficient of static friction for *Laminaria japonica-Laminaria japonica* ($COS_{L\text{-}L}$) and the coefficient of static friction for *Laminaria japonica*-steel ($COS_{L\text{-}S}$) were calculated to be 0.84 and 0.72, respectively. The average coefficient of rolling friction for *Laminaria japonica-Laminaria japonica* ($COO_{L\text{-}L}$) and the coefficient of rolling friction for *Laminaria japonica*-steel ($COO_{L\text{-}S}$) were calculated to be 0.44 and 0.36, respectively.

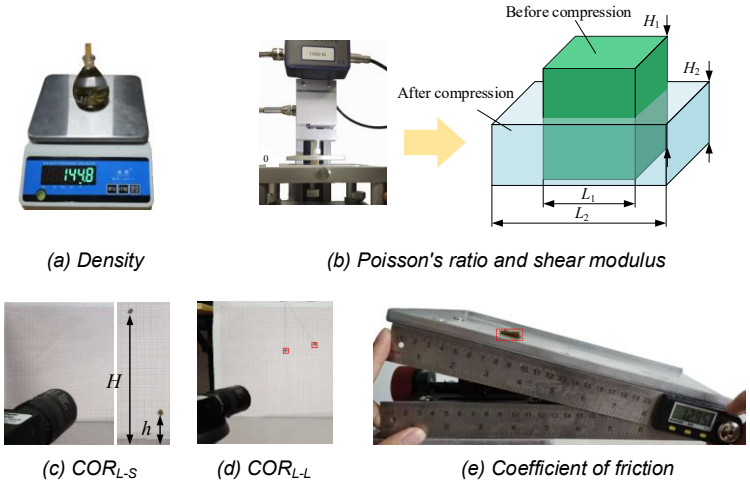

(a) Density (b) Poisson's ratio and shear modulus

(c) COR_{L-S} (d) COR_{L-L} (e) Coefficient of friction

Fig. 3 - Measurement of physical parameters of *Laminaria japonica*

Shear test

Shear test is a widely used method for determining the mechanical properties of materials and is frequently applied in the study of shear strength, rheological properties, and deformation behaviors of agricultural materials *(Li et al., 2017)*. In this study, shear test was performed using the multifunctional texture analyzer (Fig 4a). This equipment collects mechanical response data during the shear process of *Laminaria japonica* using a high-precision force-displacement sensor, making it suitable for experimental analysis of the shear mechanical properties of biological materials.

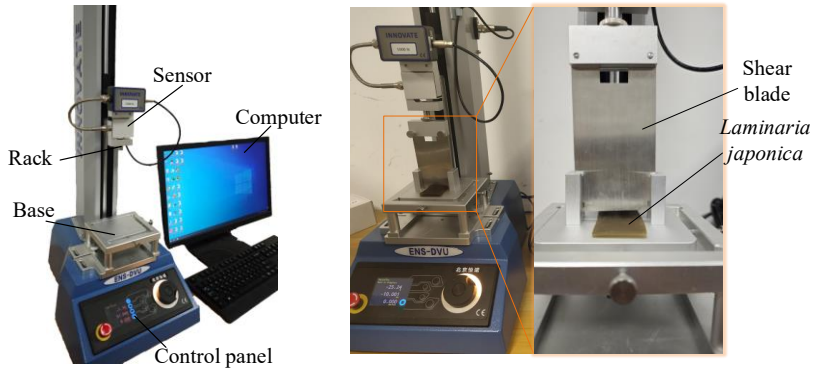

(a) Multifunctional texture analyser (b) Shearing process

Fig. 4 - Shear test of *Laminaria japonica*

A total of 30 fresh *Laminaria japonica* samples 1 were randomly selected for the shear tests. A shear blade with a thickness of 1.2 mm and a base gap of 1.5 mm, with a loading speed of 0.5 mm/s. A texture analyzer was employed to record the shear force–time curve in real time. The maximum shear force (F_{max}) of *Laminaria japonica* samples 1 with different thicknesses was measured and used as the key index for the calibration of discrete element model parameters, as shown in Fig 4b.

Particle radius and shear model construction

In the discrete element software EDEM, the behavior of the model is determined by several key parameters such as particle parameter, bonding parameters, and the computational time step. The actual thickness of *Laminaria japonica* ranges from 0.8 to 5.2 mm, and since its length is relatively large, the variation in thickness across the shear range can be considered negligible. Thus, a *Laminaria japonica* model with a thickness of its mean (3 mm) is established. To balance computational performance with simulation accuracy, uniform particles with a radius of 0.5 mm are selected as the basic particles, and a contact radius of 0.75 mm is chosen to ensure continuous bonds between particles. To ensure the accuracy of the subsequent calibration of discrete element parameters, the dimensions of the established discrete element model must match those of the physical test samples (Fig. 5). In the EDEM software, models for the shear blade and base with dimensions identical to those of the physical test are created. The discrete element model of *Laminaria japonica* sample is placed on the base, and the simulation test parameters are set to match those of the physical test (Fig 5). The detailed DEM simulation parameters are shown in Table 1.

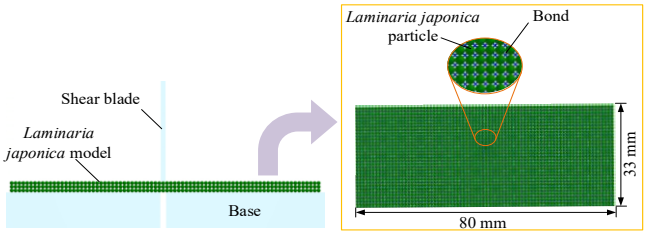

Fig. 5 - Discrete element model of *Laminaria japonica* sample

Table 1

Parameter table for *Laminaria japonica* simulated shear test

Types	Parameters	Values	Source
Intrinsic parameter	Density of *Laminaria japonica* (kg/m^3)	1263	Measurement
	Poisson's ratio of *Laminaria japonica*	0.338	Measurement
	Shear modulus of *Laminaria japonica* (MPa)	5.43	Measurement
	Density of steel (kg/m^3)	7865	*Zhang et al. (2023)*
	Poisson's ratio of steel	0.30	*Zhang et al. (2023)*
	Shear modulus of steel (GPa)	79	*Zhang et al. (2023)*
Contact parameter	$COR_{L\text{-}L}$	0.2~0.6	Calibration
	$COS_{L\text{-}L}$	0.4~1.2	Calibration
	$COO_{L\text{-}L}$	0.2~0.6	Calibration
	$COR_{L\text{-}S}$	0.3~0.7	Calibration
	$COS_{L\text{-}S}$	0.4~1.2	Calibration
	$COO_{L\text{-}S}$	0.2~0.6	Calibration
Bonding model parameters	Normal stiffness per unit area (MN/m^3)	100~900	Calibration
	Shear stiffness per unit area (MN/m^3)	100~900	Calibration
	Critical normal stress (MPa)	1~9	Calibration
	Critical shear stress (MPa)	1~9	Calibration
	Bonding radius (mm)	0.6~1	Calibration

Calibration of simulation parameters

Plackett-Burman test

In this study, Plackett-Burman test design was implemented using Design-Expert software. A total of 11 actual parameters and 8 virtual parameters were selected as experimental factors in this study. The actual parameters included: $COR_{L\text{-}L}$ (x_1), $COS_{L\text{-}L}$ (x_2), $COO_{L\text{-}L}$ (x_3), $COR_{L\text{-}S}$ (x_4), $COS_{L\text{-}S}$ (x_5), $COO_{L\text{-}S}$ (x_6), normal stiffness per unit area (x_7), shear stiffness per unit area (x_8), critical normal stress (x_9), critical shear stress (x_{10}), and bonding radius (x_{11}). Additionally, there were 8 virtual parameters (x_{12}~x_{19}). Each parameter was tested at two levels, high (+1) and low (-1). The performance indicator for the experiments was F_{max}. A total of 20 experiments were conducted. The detailed experimental design and simulation results are shown in Table 2 (columns for virtual parameters are omitted).

Table 2

Design and results of Plackett-Burman test

No.	Factors											F_{max}/N	No.	Factors										F_{max}/N
	x_1	x_2	x_3	x_4	x_5	x_6	x_7	x_8	x_9	x_{10}	x_{11}			x_1	x_2	x_3	x_4	x_5	x_6	x_7	x_8	x_9	x_{10}	x_{11}	
1	1	1	-1	-1	1	1	1	1	-1	1	-1	264.8	11	1	-1	1	-1	-1	-1	-1	1	1	-1	1	220.5
2	-1	1	1	-1	-1	1	1	1	1	-1	1	165.6	12	-1	1	-1	1	-1	-1	-1	-1	1	1	-1	42.6
3	1	-1	1	1	-1	-1	1	1	1	1	-1	304	13	1	-1	1	-1	1	-1	-1	-1	-1	1	1	133.8
4	1	1	-1	1	1	-1	-1	1	1	1	1	574.5	14	1	1	-1	1	-1	1	-1	-1	-1	-1	1	113.3
5	-1	1	1	-1	1	1	-1	-1	1	1	1	3.7	15	1	1	1	-1	1	-1	1	-1	-1	-1	-1	169.1
6	-1	-1	1	1	-1	1	1	-1	-1	1	1	321.5	16	1	1	1	1	-1	1	-1	1	-1	-1	-1	174.9
7	-1	-1	-1	1	1	-1	1	1	-1	-1	1	530	17	-1	1	1	1	1	-1	1	-1	1	-1	-1	170.3
8	-1	-1	-1	-1	1	1	-1	1	1	-1	-1	195.7	18	-1	-1	1	1	1	1	-1	1	-1	1	-1	259.4
9	1	-1	-1	-1	-1	1	1	-1	1	1	-1	116.5	19	1	-1	-1	1	1	1	1	-1	1	-1	1	264.8
10	-1	1	-1	-1	-1	-1	1	1	-1	1	1	388.7	20	-1	-1	-1	-1	-1	-1	-1	-1	-1	-1	-1	165.6

Steepest climb test

Based on the significant parameters selected from the Plackett-Burman test, a steepest climb test was conducted to further narrow the effective range of these parameters and quickly approach optimal values. Five groups of steepest climb test were designed, with the non-significant parameters set to their intermediate values.

Box-Behnken test

To establish a mathematical model between F_{max} and the discrete element simulation parameters in the simulation tests, and to find the optimal parameters for the *Laminaria japonica* model, Box-Behnken test designs were employed based on the results of the steepest climb test. This approach used a four-factor, three-level design to optimize significant parameters. The specific design and results of Box-Behnken test are shown in Table 3.

Table 3

Design and results of Box-Behnken test

No.	Factors				F_{max}/N	No.	Factors				F_{max}/N
	x_4	x_7	x_8	x_{11}			x_4	x_7	x_8	x_{11}	
1	0.4	0.6	0.4	0.8	122.8	16	0.5	1	0.5	0.8	226.5
2	0.6	0.6	0.4	0.8	143.6	17	0.4	0.8	0.3	0.8	100.6
3	0.4	1	0.4	0.8	178.3	18	0.6	0.8	0.3	0.8	102.2
4	0.6	1	0.4	0.8	206.5	19	0.4	0.8	0.5	0.8	186.2
5	0.5	0.8	0.3	0.7	73.5	20	0.6	0.8	0.5	0.8	221.7
6	0.5	0.8	0.5	0.7	167.8	21	0.5	0.6	0.4	0.7	106.4
7	0.5	0.8	0.3	0.9	135.4	22	0.5	1	0.4	0.7	155.5
8	0.5	0.8	0.5	0.9	236.5	23	0.5	0.6	0.4	0.9	159.2
9	0.4	0.8	0.4	0.7	128	24	0.5	1	0.4	0.9	226.1
10	0.6	0.8	0.4	0.7	142.5	25	0.5	0.8	0.4	0.8	170.1
11	0.4	0.8	0.4	0.9	177.9	26	0.5	0.8	0.4	0.8	168.2
12	0.6	0.8	0.4	0.9	211.4	27	0.5	0.8	0.4	0.8	158.2
13	0.5	0.6	0.3	0.8	66.4	28	0.5	0.8	0.4	0.8	168.8
14	0.5	1	0.3	0.8	131.6	29	0.5	0.8	0.4	0.8	167.9
15	0.5	0.6	0.5	0.8	173.3	-	-	-	-	-	-

Regression prediction of F_{max} based on the GP-PSO-XGBoost model

According to the analysis results of the Plackett-Burman and Box-Behnken tests, four factors (x_4, x_7, x_8, and x_{11}) were identified as having significant effects on F_{max}, with notable interactions observed among them. A GP-PSO-XGBoost regression prediction model was developed in the Python environment, integrating the eXtreme Gradient Boosting (XGBoost) algorithm with two heuristic optimization methods: Particle Swarm Optimization (PSO) and Gaussian Process-based Bayesian Optimization. This hybrid approach was designed to enhance both the model's capacity to capture complex data patterns and its nonlinear modeling capability. To further expand the feature space, second-order and interaction terms were generated using the Polynomial Features function.

In the GP-PSO-XGBoost model, x_4, x_7, x_8, and x_{11} were selected as input features, with F_{max} as the output target. Bayesian optimization was employed for global exploration in the parameter space, while PSO performed local search through iterative updates within the particle population, improving both the convergence speed and the robustness of the model. The hybrid optimization process is illustrated in Fig 6. Experimental data were divided into 60% for training, 20% for validation, and 20% for testing. The model performance was evaluated using the coefficient of determination R^2, R^2_{Adj}, and MAPE.

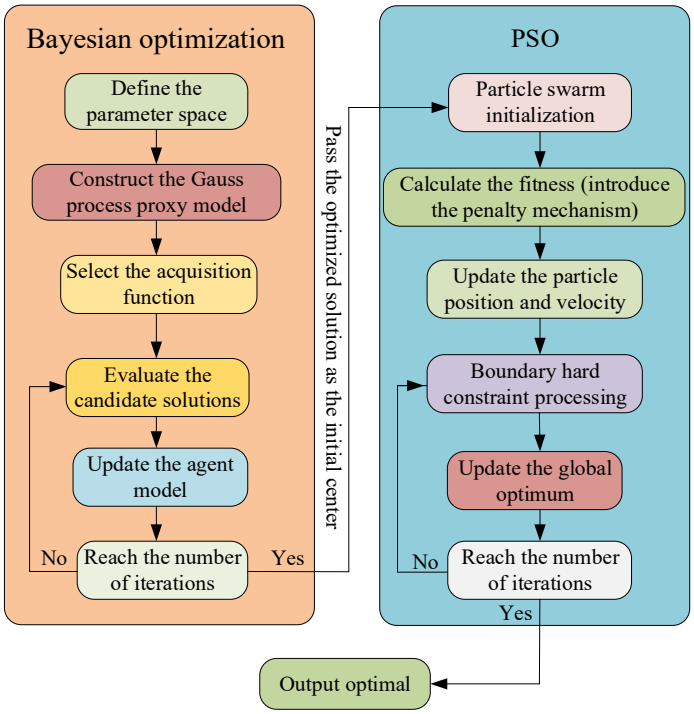

Fig. 6 - Hybrid optimization process

Validation of the Laminaria japonica model

To evaluate the accuracy of the calibrated model, experimental verification was conducted based on the prediction results of the GP-PSO-XGBoost model. Discrete element models of *Laminaria japonica* with different thicknesses were established, and their accuracy was assessed by comparing the simulation results with the predictions derived from the fitted equation. Puncture tests were further utilized for physical and simulation comparative analysis. The deformation and stress states of *Laminaria japonica* observed during the simulation were compared with those recorded in the physical tests. This comparison allowed for an assessment of the model's predictive accuracy, ensuring that the calibrated and optimized model delivers reliable and accurate results for practical applications.

Shear validation of Laminaria japonica models with different thicknesses

Based on the optimized parameters, discrete element models of *Laminaria japonica* with thicknesses of 1, 2, 3, 4, and 5 mm were constructed, and simulated shear tests were conducted for comparative validation against the equation fitting results.

Verification of puncture test results

To evaluate the adaptability of the discrete element model of *Laminaria japonica*, both physical and simulated puncture tests were conducted on *Laminaria japonica* sample 1 with a thickness of 3 mm and the corresponding discrete element model. In the physical test, the sample was placed on the base of the texture analyzer, ensuring that the sample was flat. The puncture probe of the texture analyzer moved downwards at a constant speed of 0.5 mm/s until it completely penetrated the sample *(Chen et al., 2024)*. The puncture force-displacement curves were recorded. The simulation tests were conducted under identical parameters.

RESULTS AND DISCUSSION

Shear test

Since the thickness of *Laminaria japonica* is not completely uniform, to obtain the corresponding F_{max} for the thickness (3 mm) of the *Laminaria japonica* discrete element model, a fitting relationship between thickness and F_{max} was established. First, data from 30 groups of *Laminaria japonica* shear tests were imported into Origin software to obtain the relationship between *Laminaria japonica* thickness and F_{max}. The fitted relationship curve is shown in Fig. 7, which approximates a linear relationship.

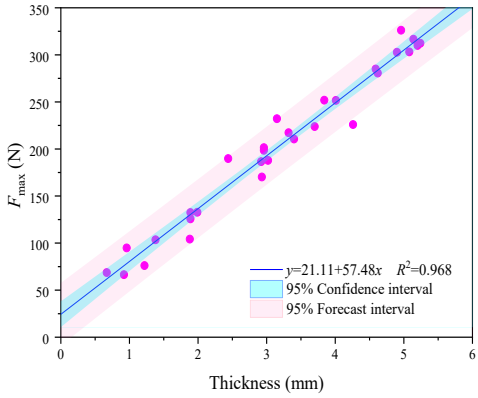

Fig. 7 - Relationship of F_{max}-thickness of *Laminaria japonica*

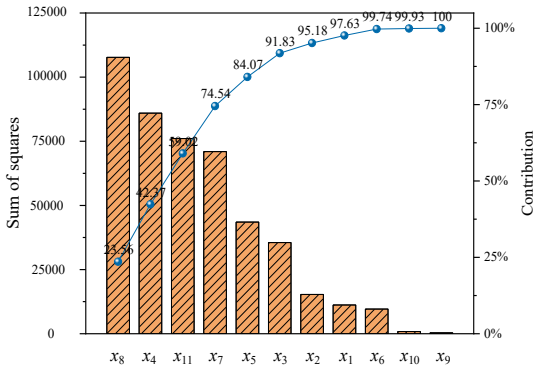

Fig. 8 - Pareto chart

Observations of the *Laminaria japonica* samples of 1 revealed that as the thickness of the *Laminaria japonica* increased, the internal structural organization increased, allowing it to withstand greater external forces. Additionally, the shear results indicated that F_{max} gradually increased with the thickness of the *Laminaria japonica*. Most of the data points for sample thickness and F_{max} fell within the 95% confidence interval, indicating that the fitted equation derived from the sample data was reliable. This equation can predict the F_{max} required for shear test of *Laminaria japonica* at various thicknesses. In the discrete element parameter calibration test, a *Laminaria japonica* model with a thickness of 3 mm was used. Substituting this thickness into the fitting equation yielded an F_{max} of 193.55 N.

Plackett-Burman test

After conducting an ANOVA on the experimental results, the significance effect of the 11 actual parameters on F_{max} was obtained. The Pareto chart visually illustrates the degree of influence of each factor, as shown in Fig 8. For cases with significant parameter variation, $COR_{L\text{-}S}$ (x_4), normal stiffness per unit area (x_7), bonding radius (x_{11}) and shear stiffness per unit area (x_8) collectively contributed to 75.54% of the total influence on F_{max}. These four parameters were found to have a significant effect on F_{max}, whereas the influence of the other parameters was relatively minor.

To further refine the range of significant parameters, steepest climb test and Box-Behnken test were employed in subsequent experiments. These experiments focused on the four significant parameters identified, while the remaining parameters, which showed no significant effect, were set to intermediate levels. The specific parameter settings were as follows: x_1=0.4, x_2=0.8, x_3=0.4, x_5=0.8, x_6=0.4, x_9=5 MPa, x_{10}=5 MPa.

Steepest climb test

The design and results of steepest climb test are shown in Table 4. According to the fitting equation, F_{max} was calculated to be 193.55 N for a *Laminaria japonica* thickness of 3 mm. This calculated value was compared with the simulation results to determine the percentage error.

The results of the steepest climb test showed that as x_4, x_7, x_8, and x_{11} increased, the F_{max} for *Laminaria japonica* also increased accordingly. The errors between the simulation and physical tests initially showed a decreasing trend, followed by an increasing trend. To further find the optimal parameter combination, the parameter settings from test 2 were used as the center point for subsequent tests, with tests 1 and 3 serving as references for low and high levels, respectively.

Table 4

Design and results of steepest climb test

No.	Factors				F_{max}/N	Error/%
	x_4	x_7	x_8	x_{11}		
1	0.3	100	100	0.6	48.3	-75.05
2	0.4	300	300	0.7	168.9	-12.74
3	0.5	500	500	0.8	305.7	57.94
4	0.6	700	700	0.9	435.0	124.75
5	0.7	900	900	1.0	460.4	137.87

Box-Behnken test

Based on the test results, ANOVA was conducted using the analysis fitting module in Design-Expert software, resulting in a quadratic regression equation with F_{max} as the response variable and x_4, x_7, x_8, and x_{11} as variables. This equation can predict the F_{max} based on these discrete element parameters. The fitted quadratic regression equation is as follows:

$$\begin{aligned} Y = {} & 166.64 + 11.17x_4 + 29.40x_7 + 50.19x_8 + 31.07x_{11} + 1.85x_4x_7 \\ & + 8.47x_4x_8 + 4.75x_4x_{11} - 3.00x_7x_8 + 4.45x_7x_{11} + 1.70x_8x_{11} - 0.60{x_4}^2 \\ & - 3.79{x_7}^2 - 13.10{x_8}^2 - 0.79{x_{11}}^2 \end{aligned} \quad (5)$$

To validate the accuracy of the quadratic regression model, residual analysis was performed. The normal probability plot of the residuals shows that the points are almost distributed along a straight line, indicating that the residuals are close to a normal distribution. Additionally, by comparing the actual and predicted values, it was found that most of the data points lie close to a straight line, further confirming the predictive accuracy of the model, as shown in Fig 9 and Fig 10. Therefore, the fitted quadratic regression model is accurate and reliable *(Awuah et al., 2022)*.

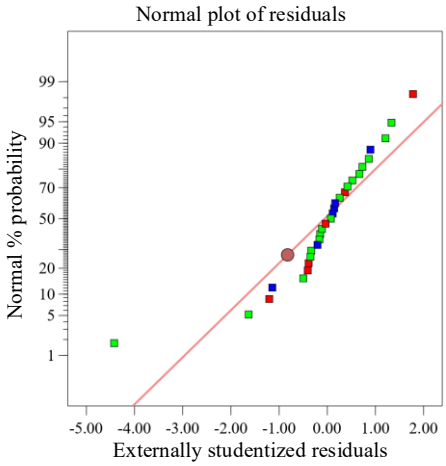

Fig. 9 - Residual normal distribution diagram

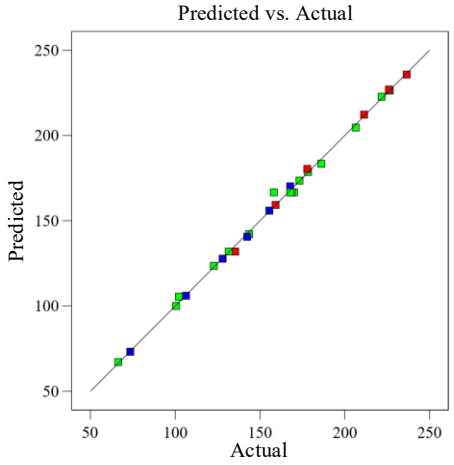

Fig. 10 - Correspondence between predicted value and actual value

From the ANOVA (Table 5), it was determined that the model was extremely significant statistical significance (P<0.0001), and the lack of fit was not significant. The model's R^2 value of 0.9973 and adjusted R^2_{Adj}value of 0.9947 indicated an excellent fit, effectively accounting for the variability in the data. ANOVA further indicated that x_4, x_7, x_8, x_{11}, x_4x_8, and ${x_8}^2$ had extremely significant effects on F_{max} (P<0.01), while x_4x_{11}, x_7x_{11}, and ${x_7}^2$ had significant effects (P<0.05).

Table 5

ANOVA of Box-Behnken test

Source	Sum of Squares	df	Mean Square	F-value	P-value
Model	55374.52	14	3955.32	373.71	< 0.0001
x_4	1498.57	1	1498.57	141.59	< 0.0001**
x_7	10372.32	1	10372.32	980.00	< 0.0001**
x_8	30230.44	1	30230.44	2856.24	< 0.0001**
x_{11}	11581.65	1	11581.65	1094.26	< 0.0001**
x_4x_7	13.69	1	13.69	1.29	0.2745
x_4x_8	287.30	1	287.30	27.14	0.0001**
x_4x_{11}	90.25	1	90.25	8.53	0.0112*
x_7x_8	36.00	1	36.00	3.40	0.0864
x_7x_{11}	79.21	1	79.21	7.48	0.0161*
x_8x_{11}	11.56	1	11.56	1.09	0.3137
${x_4}^2$	2.36	1	2.36	0.22	0.644
${x_7}^2$	93.21	1	93.21	8.81	0.0102*
${x_8}^2$	1113.71	1	1113.71	105.23	< 0.0001**
${x_{11}}^2$	4.06	1	4.06	0.38	0.5458
Residual	148.18	14	10.58		

Source	Sum of Squares	df	Mean Square	F-value	P-value
Lack of Fit	56.28	10	5.63	0.24	0.9676
Pure Error	91.89	4	22.97		
Cor Total	55522.70	28			
R^2=0.9973		R^2_{Adj}=0.9947			

*Note: * means significant difference (P<0.05), ** means extremely significant difference (P<0.01).*

Prediction results of the GP-PSO-XGBoost model

The predictive performance of the GP-PSO-XGBoost model is shown in Table 6. These results demonstrate that the model possesses excellent fitting performance and high generalization capability, with no signs of overfitting or underfitting. The XGBoost model, enhanced by the hybrid optimization framework, exhibits robust performance, delivering high accuracy, strong robustness, and remarkable generalization even under small-sample conditions. This provides a novel and effective framework for prediction and parameter optimization in future experimental studies.

Table 6

Comparison of model evaluation indicators

Evaluation type	Training set	Validation set	Test set
R^2	0.9991	0.9544	0.9727
R^2_{Adj}	0.9998	0.9895	0.9937
MAPE	0.57%	4.08%	3.16%

The result of parameter calibration

Prediction of optimal parameters for the *Laminaria japonica* shear model was made using the GP-PSO-XGBoost model. As a result, the optimal discrete element parameter combination for the *Laminaria japonica* model was determined as follows: CORL-S of 0.45, normal stiffness per unit area of 303 MN/m^3, shear stiffness per unit area of 378 MN/m^3, and bonding radius of 0.70 mm. Non-significant factors were assigned intermediate values. The final optimized discrete element parameters of the *Laminaria japonica* model are shown in Table 7.

Table 7

The final parameter calibration results of the discrete element model of *Laminaria japonica*

Factors	Parameters	Values
x_1	$COR_{L\text{-}L}$	0.40
x_2	$COS_{L\text{-}L}$	0.80
x_3	$COO_{L\text{-}L}$	0.40
x_4	$COR_{L\text{-}S}$	0.45
x_5	$COS_{L\text{-}S}$	0.80
x_6	$COO_{L\text{-}S}$	0.40
x_7	Normal stiffness per unit area (MN/m^3)	303
x_8	Shear stiffness per unit area (MN/m^3)	378
x_9	Critical normal stress (MPa)	500
x_{10}	Critical shear stress (MPa)	500
x_{11}	Bonding radius (mm)	0.70

Verification of parameter calibration results

The optimal combination of parameters was assigned to the discrete element model of *Laminaria japonica* with a thickness of 3 mm, and shear test was conducted under the same conditions. The measured F_{max} was 192.10 N, with a relative error of 0.75% compared to the fitted value (193.55 N), demonstrating close agreement between the simulation results and the fitted values. The simulation validation test was compared with the physical shear test of *Laminaria japonica* with a thickness of 3.02 mm (the closest experimental value to 3 mm). The shear force-displacement curves for both were extracted, as shown in Fig 11. The results showed high consistency in the shear force-displacement curves and deformation processes between the two tests. The *Laminaria japonica* samples of 1 in the shear tests exhibited three typical stages: (I) elastic stage, (II) local fracture stage, and (III) complete fracture stage.

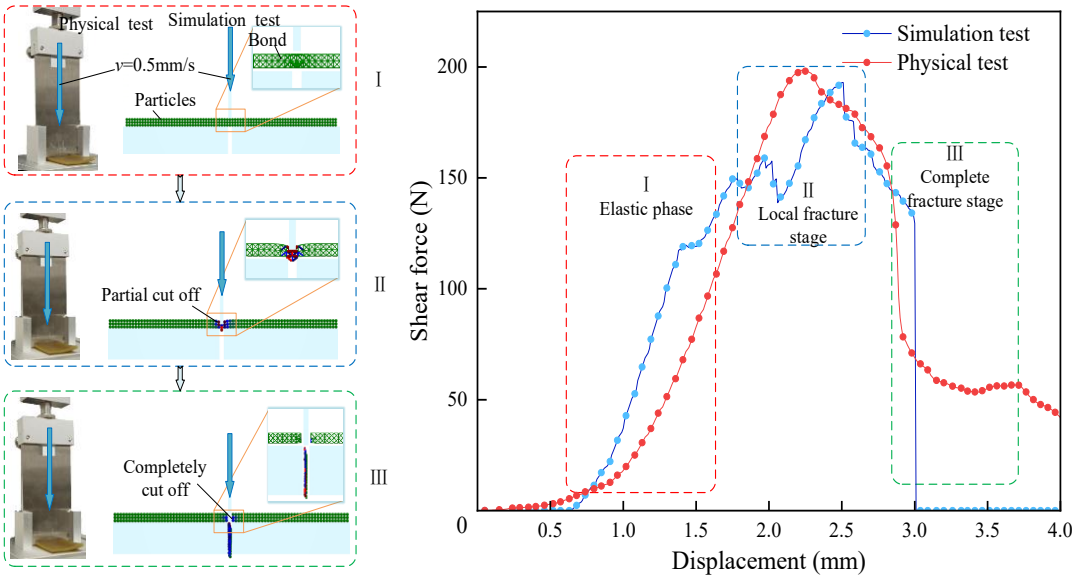

Fig. 11 - Shear test process and shear force-displacement curves

During both the simulated and physical shear test, as the shear blade moved downwards and compressed the surface of the *Laminaria japonica*, the shear force gradually increased, displaying a linear relationship with displacement within the elastic deformation range. The samples effectively resisted external forces, exhibiting prominent elastic properties (Stage I). As the shear blade continued its downward motion, the shear force increased further, and the sample began to fracture (with the bonds gradually stretching until rupture). At this stage, the internal structure of the *Laminaria japonica* began to deteriorate, with the shear force peaking and then starting to decline (Stage II). With continued displacement, the overall structure of the *Laminaria japonica* was completely compromised (the bonds were fully severed), leading to a rapid reduction in shear force as the sample lost its ability to resist external forces (Stage III). It is important to note that in the simulation test, the final shear force dropped to 0, whereas in the physical test, a residual force was observed. This discrepancy arises because the model in the simulation was cleanly cut by the shear blade, resulting in no further interaction with the blade after the cut (Fig. 12). Conversely, in the physical test, the *Laminaria japonica* was not cut neatly, it was divided into two segments that continued to interact with the shear blade, generating frictional forces and thus maintaining a residual shear force.

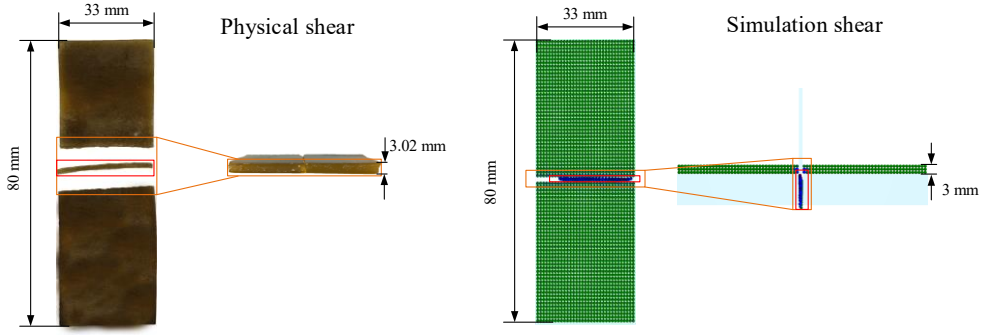

Fig. 12 - Samples after shear test

Shear validation of Laminaria japonica models with different thicknesses

The F_{max} errors of the *Laminaria japonica* models at different thicknesses are shown in Fig. 13. The average relative error across all models was 3.09%, with the maximum error occurring at a thickness of 5 mm, reaching 8.75%. This discrepancy is likely attributed to the increased complexity of the mechanical behavior in thicker samples, where pronounced non-uniformity or variations in bonding force distribution may arise. Nevertheless, the simulated predictive errors remain within an acceptable range. This indicates that the calibrated *Laminaria japonica* model exhibits excellent shear performance and adaptability. The model provides a reliable foundation for future research into the mechanical properties of *Laminaria japonica* and development of harvesting equipment for this species.

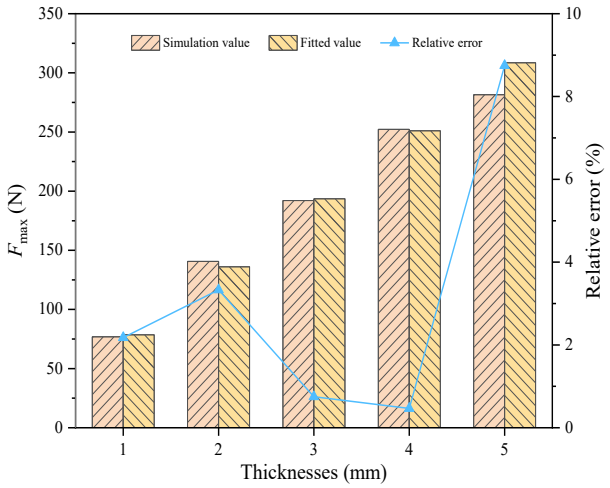

Fig. 13 - Relative error of F_{max} for different thickness models

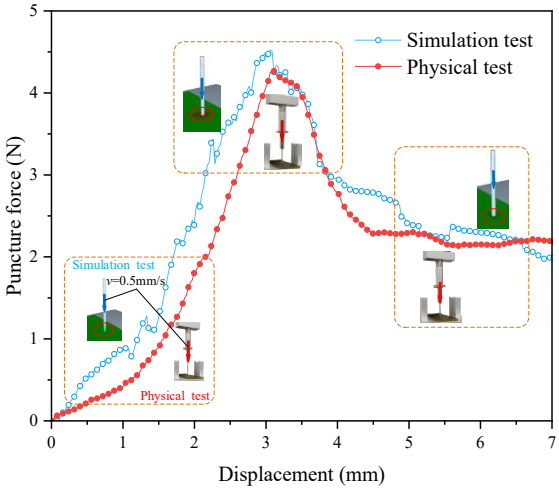

Fig. 14 - Puncture force-displacement curves

Verification of puncture test results

The puncture force-displacement curves for both simulation and physical tests are shown in Fig 14. A comparison of the two tests reveals that the overall trends of the puncture force-displacement curves are consistent. Both the simulation and physical tests indicate that as displacement increases, the force acting on the probe increases approximately linearly, reaching its maximum value when the probe fully penetrates the sample. The relative error at this point is 5.59%, suggesting a small error and strong agreement between the model and the *Laminaria japonica* samples. However, the simulation puncture force-displacement curve exhibits slight fluctuations compared to the physical test. This discrepancy is likely due to the larger particle radius used in the simulation model, which may introduce delays in the force response and slight oscillations during the transfer of collision forces between particles.

In summary, the established *Laminaria japonica* shear model effectively captures the mechanical properties of real *Laminaria japonica*, exhibiting strong predictive performance and accurately simulating the stress behavior of *Laminaria japonica* during mechanical harvesting. However, the mechanical properties of *Laminaria japonica* at the microscopic level are more complex. The model's assumptions about particle bonding may oversimplify these complexities. Future improvements in computational power are necessary to enhance calculation efficiency and enable further optimization of the model's microscopic parameters.

Establishment of the overall discrete element model for Laminaria japonica

Observations of a large number of *Laminaria japonica* samples revealed that its morphology is greatly influenced by the growth environment, especially in the edge regions. However, its thickness distribution generally follows a pattern of being thicker in the middle and thinner at the edges. To simplify the model, this study approximated *Laminaria japonica* as a flat structure while preserving its characteristic thickness distribution. Based on the Discrete Element Method (DEM), the model was filled with particles to generate a complete DEM model of *Laminaria japonica*, as shown in Fig. 15. This simplified design aims to provide a reference for mechanical harvesting and to lay the foundation for subsequent simulation tests and physical validation.

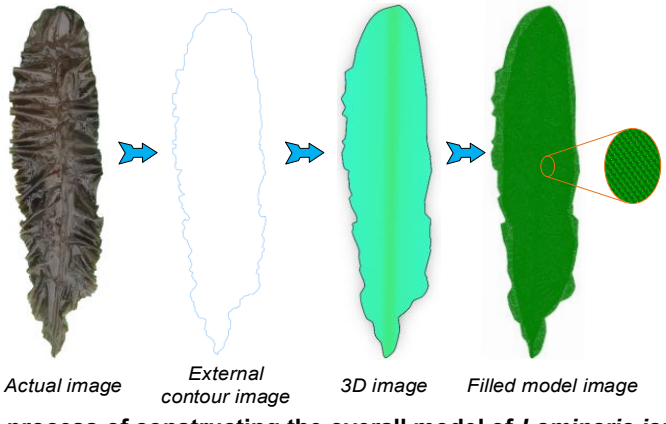

Fig. 15 - The process of constructing the overall model of *Laminaria japonica*

CONCLUSIONS

The physical, contact, and mechanical properties of Laminaria japonica were measured through physical experiments. Based on the Hertz-Mindlin with bonding model, a discrete element model of Laminaria japonica was developed by combining physical and simulation tests. Model parameter calibration was carried out, and the optimal parameter combination was obtained and validated. Using the F_{max} as the test indicator, the optimal parameters were obtained through Plackett-Burman test, the steepest climb test, Box-Behnken test, and the GP-PSO-XGBoost regression prediction model. The results indicated that when the coefficient of restitution of *Laminaria japonica*-steel was 0.45, the normal stiffness per unit area was 303 MN/m^3, the shear stiffness per unit area was 378 MN/m^3, and the bonding radius was 0.70 mm, the relative error of F_{max} was 0.75%. The average error of F_{max} across different thicknesses was 3.09%, and the relative error in maximum puncture force was 5.59%. These results demonstrate that the GP-PSO-XGBoost hybrid optimization and regression prediction model effectively captures complex inter-factor relationships, improves prediction accuracy and reliability, and provides strong support for parameter optimization in discrete element simulations. The discrete element model developed in this study lays a foundation for the design and optimization of Laminaria japonica harvesting equipment.

ACKNOWLEDGMENTS

This work was financially supported by the Key R&D Program Project in Shandong Province (Grant No. 2022CXGC020410).

REFERENCES

[1] Awuah, E., Zhou, J., Lian, Z. A., Aikins, K. A., Gbenontin, B. V., Mecha, P., & Makange, N. R. (2022). Parametric analysis and numerical optimisation of Jerusalem artichoke vibrating digging shovel using discrete element method. *Soil & Tillage Research*, 219, 105344. https://doi.org/10.1016/j.still.2022.105344

[2] Chang, Z., Zhang, Y., Zheng, Z., Wan, R., & Zhang, Z. (2018). Development status of the raft-cultivation harvesting devices for Laminaria japonica (筏式养殖海带收获装置的发展现状). *Fishery Modernization*, 45(1), 40-48. https://doi.org/10.3969/j.issn.1007-9580.2018.01.007 (in Chinese).

[3] Chen, H., Jin, L., Fang, C., Liu, L., Kačániová, M., Wang, J., Lu, J., & Ban, Z. (2024). Integration of puncture loading and finite element simulations to predict the mechanical responses for kiwifruit. *Postharvest Biology and Technology*, 217, 113102. https://doi.org/10.1016/j.postharvbio.2024.113102

[4] Gao, X., Xie, G., Li, J., Shi, G., Lai, Q., & Huang, Y. (2023). Design and validation of a centrifugal variable-diameter pneumatic high-speed precision seed-metering device for maize. *Biosystems Engineering*, 227, 161-181. https://doi.org/10.1016/j.biosystemseng.2023.02.004

[5] Guo, J., Karkee, M., Yang, Z., Fu, H., Li, J., Jiang, Y., Jiang, T., Liu, E., & Duan, J. (2021). Discrete element modeling and physical experiment research on the biomechanical properties of banana bunch stalk for postharvest machine development. *Computers and Electronics in Agriculture*, 188, 106308. https://doi.org/10.1016/j.compag.2021.106308

[6] He, B., Ming, Y., Pu, Y., Sun, Y., Jin, M., Yu, C., & Qi, H. (2020). The dual effects of riboflavin and Laminaria japonica polyphenol extracts on the gel properties of myofibrillar protein from Scomberomorus Niphonius under UVA irradiation. *Food Chemistry*, 332, 127373. https://doi.org/10.1016/j.foodchem.2020.127373

[7] Jiang, T., Hong, Y., Lu, L., Zhu, Y., Chen, Z., & Yang, M. (2022). Design and experiment of a new mode of mechanized harvesting of raft cultured Laminaria japonica. *Aquacultural Engineering*, 99, 102289. https://doi.org/10.1016/j.aquaeng.2022.102289

[8] Li, J., Bergman, K., Thomas, J., Gao, Y., & Gröndahl, F. (2023). Life Cycle Assessment of a large commercial Laminaria japonica farm in Shandong. *Science of The Total Environment*, 903, 166861. https://doi.org/10.1016/j.scitotenv.2023.166861

[9] Li, M., Xu, S., Yang, Y., Guo, L., & Tong, J. (2017). A 3D simulation model of corn stubble cutting using finite element method. *Soil & Tillage Research*, 166, 43-51. https://doi.org/10.1016/j.still.2016.10.003

[10] Li, S., Diao, P., Miao, H., Zhao, Y., Li, X., & Zhao, H. (2024). Modeling the fracture process of wheat straw using a discrete element approach. *Powder Technol*, 439, 119726. https://doi.org/10.1016/j.powtec.2024.119726

[11] Naylor, R. L., Hardy, R. W., Buschmann, A. H., Bush, S. R., Cao, L., Klinger, D. H., Little, D. C., Lubchenco, J., Shumway, S. E., & Troell, M. (2021). A 20-year retrospective review of global aquaculture. *Nature*, 591, 551-563. https://doi.org/10.1038/s41586-021-03308-6

[12] Tan, Y., Lou, S., & Chen, Z. (2020). Research on integrated specialized ship for Laminaria japonica harvesting, classifying and grading. *Aquacultural Engineering*, 91, 102121. https://doi.org/10.1016/j.aquaeng.2020.102121

[13] Tang, H., Xu, F., Xu, C., Zhao, J., & Wang, Y. (2023). The influence of a seed drop tube of the inside-filling air-blowing precision seed-metering device on seeding quality. *Computers and Electronics in Agriculture*, 204, 107555. https://doi.org/10.1016/j.compag.2022.107555

[14] Tian, Y., Zeng, Z., Gong, H., Zhou, Y., Qi, L., & Zhen, W. (2023). Simulation of tensile behavior of tobacco leaf using the discrete element method (DEM). *Computers and Electronics in Agriculture*, 205, 107570. https://doi.org/10.1016/j.compag.2022.107570

[15] Wachem, B., Thalberg, K., Nguyen, D., Juan, L., Remmelgas, J., & Niklasson-Bjorn, I. (2020). Analysis, modelling and simulation of the fragmentation of agglomerates. *Chemical Engineering Science*, 227, 115944. https://doi.org/10.1016/j.ces.2020.115944

[16] Zhang, Z., Mei, F., Xiao, P., Zhao, W., & Zhu, X. (2023). Discrete element modelling and simulation parameters calibration for the compacted straw cube. *Biosystems Engineering*, 230, 301-312. https://doi.org/10.1016/j.biosystemseng.2023.04.019

[17] Zhao, S., Pan, Z., Azarakhsh, N., Ramaswamy, H., Duan, H., & Wang, C. (2024). Effects of high-pressure processing on the physicochemical and adsorption properties, structural characteristics, and dietary fiber content of Laminaria japonica (Laminaria japonica), *Current Research in Food Science*, 8, 100671. https://doi.org/10.1016/j.crfs.2023.100671

[18] Zhao, J., Zhao, S., & Luding, S. (2023). The role of particle shape in computational modelling of granular matter. *Nature Reviews Physics*, 5(9), 505-525. https://doi.org/10.1038/s42254-023-00617-9